

UC Riverside

UC Riverside Previously Published Works

Title

The Nature of the Hydrated Proton H(aq) + in Organic Solvents

Permalink

<https://escholarship.org/uc/item/2jp3w86j>

Journal

Journal of the American Chemical Society, 130(36)

ISSN

0002-7863

Authors

Stoyanov, Evgenii S
Stoyanova, Irina V
Tham, Fook S
et al.

Publication Date

2008-09-10

DOI

10.1021/ja803535s

Peer reviewed

The Nature of the Hydrated Proton $H_{(aq)}^+$ in Organic Solvents

Evgenii S. Stoyanov,* Irina V. Stoyanova, Fook S. Tham, and Christopher A. Reed*

Department of Chemistry, University of California, Riverside, California 92521

Received May 16, 2008; E-mail: evgenii.stoyanov@ucr.edu; chris.reed@ucr.edu

Abstract: The nature of $H(H_2O)_n^+$ cations for $n = 3-8$ with weakly basic carborane counterions has been studied by IR spectroscopy in benzene and dichloroethane solution. Contrary to general expectation, neither Eigen-type $H_3O \cdot 3H_2O^+$ nor Zundel-type $H_5O_2^+ \cdot 4H_2O$ ions are present. Rather, the core species is the $H_7O_3^+$ ion.

Introduction

The current state of knowledge of the aquated proton $H_{(aq)}^+$ is in a curious position. In water, the “excess proton” is widely believed to exist in two limiting forms, the Eigen-type H_3O^+ ion¹ and the Zundel-type $H_5O_2^+$ ion,² coexisting in a dynamic equilibrium. These ions are well characterized in crystalline salts,^{3,4} organic solvents,⁵⁻⁷ and the gas phase,⁸⁻¹⁰ but the extent to which they represent $H_{(aq)}^+$ in water has not been determined experimentally. The belief that $H_{(aq)}^+$ is an approximately 60:40 ratio of hydrated Eigen:Zundel ions is based on theory.^{11,12}

The problem of developing an accurate molecular description of H^+ in water lies in the difficulty of accurately separating its spectroscopic signature(s) from those of the background water, and in interpreting the resulting spectra. Infrared is the spectroscopy of choice because of its sensitivity and fast time scale, but the IR spectrum of $H_{(aq)}^+$ is notoriously broad. A poorly understood continuous broad absorption associated with the vibrations of the excess proton extends over the much of the useful IR range. These difficulties have shifted attention to the gas phase. The underlying assumption is that an accurate molecular description of each ion-selected hydrate $H(H_2O)_n^+$ via step-by-step increasing n will ultimately lead to an understanding of $H_{(aq)}^+$ in bulk water. Indeed, experiment and theory *in vacuo* come together very nicely to establish that the trihydrated Eigen ion ($H_9O_4^+$, i.e., $H_3O^+ \cdot 3H_2O$) and the tetrahydrated Zundel ion ($H_{13}O_6^+$, i.e., $H_5O_2^+ \cdot 4H_2O$) have extra

stability in the gas phase.^{13,14} Other “magic number” clusters such as $H(H_2O)_{21}^+$ have distinctive structural characteristics and heightened stability compared to their near n neighbors.¹⁵⁻¹⁸

While gas-phase studies have obvious and direct importance in atmospheric chemistry, there are reasons to doubt that such a close relationship will hold in condensed phases — where so much acid chemistry is carried out. Gas-phase ion chemistry (and theory) is carried out in the absence of counterions, whereas all condensed-phase chemistry must deal with the necessity of a conjugate base. Even strong acids that fully ionize in a solvent are subject to ion pairing. The unidirectional electric field created by the proximity of an anion will affect the structures of the $H(H_2O)_n^+$ cations. Structural isomers of $H(H_2O)_n^+$ for $n = 5-8$ are calculated *in vacuo* to be very close in energy,^{10,19-22} so their structures should be quite sensitive to environmental influences in condensed media.

In the solid state, X-ray crystal structures of hydrated acids were studied quite extensively in the late 1970s.²³ In favorable circumstances, they can be expected to reflect the structures of ions in other phases. For example, if an $H(H_2O)_n^+$ ion is surrounded in a crystal by a spherically symmetric anion field, it might be expected to reflect the gas-phase structure of the cation. In anion fields of lower symmetry, an $H(H_2O)_n^+$ ion might be expected to reflect ion-paired structures of hydrated acids in solution.

- (1) Eigen, M. *Angew. Chem., Int. Ed. Engl.* **1964**, *3*, 1-19.
- (2) Zundel, G.; Metzger, H. *Z. Phys. Chem.* **1968**, *58*, 225-241.
- (3) Ortwein, R.; Schmidt, A. *Z. Anorg. Allg. Chem.* **1976**, *425*, 10-16.
- (4) Jones, D. J.; Roziere, J. *J. Mol. Struct.* **1989**, *195*, 283-291.
- (5) Stoyanov, E. S.; Kim, K.-C.; Reed, C. A. *J. Am. Chem. Soc.* **2006**, *128*, 1948-1958.
- (6) Stoyanov, E. S.; Smirnov, I. V.; Fedotov, M. A. *J. Phys. Chem. A* **2006**, *110*, 9505-9512.
- (7) Stoyanov, E. S.; Reed, C. A. *J. Phys. Chem. A* **2006**, *110*, 12992-13002.
- (8) Okumura, M.; Yen, L. I.; Myers, J. D.; Lee, Y. T. *J. Phys. Chem.* **1990**, *94*, 3416-3424.
- (9) Roscioli, J. R.; McCunn, L. R.; Johnson, M. A. *Science* **2007**, *316*, 249-254, and references therein.
- (10) Headrick, J. M.; Diken, E. G.; Walters, R. S.; Hammer, N. I.; Christie, R. A.; Cui, J.; Myshakin, E. M.; Duncan, M. A.; Johnson, M. A.; Jordan, K. D. *Science* **2005**, *308*, 1765-1769, and references therein.
- (11) Tuckerman, M.; Laasonen, K.; Sprik, M.; Parinello, M. J. *J. Chem. Phys.* **1995**, *103*, 150-161.
- (12) Voth, G. A. *Acc. Chem. Res.* **2006**, *39*, 143-150, and references therein.

- (13) Grimsrud, E. P.; Kebarle, P. *J. Am. Chem. Soc.* **1973**, *95*, 7939-7943.
- (14) Mizuse, K.; Fujii, A.; Mikami, N. *J. Chem. Phys.* **2007**, *126*, 231101-4, and references therein.
- (15) Searcy, J. Q.; Fenn, J. B. *J. Chem. Phys.* **1974**, *61*, 5282-5288.
- (16) Zwier, T. S. *Science* **2004**, *304*, 1119-1120.
- (17) Shin, J.-W.; Hammer, N. I.; Diken, E. G.; Johnson, M. A.; Walters, R. S.; Jaeger, T. D.; Duncan, M. A.; Christie, R. A.; Jordan, K. D. *Science* **2004**, *304*, 1137-1140.
- (18) Miyazaki, M.; Fujii, A.; Ebata, T.; Mikami, N. *Science* **2004**, *304*, 1134-1137.
- (19) Jiang, J.-C.; Wang, Y.-S.; Chang, H.-C.; Lin, S. H.; Lee, Y. T.; Niedner-Schatteburg, G.; Chang, H.-C. *J. Am. Chem. Soc.* **2000**, *122*, 1398-1410.
- (20) Christie, R. A.; Jordan, K. D. *J. Phys. Chem. A* **2001**, *105*, 7551-7558.
- (21) Wei, D.; Salahub, D. R. *J. Chem. Phys.* **1994**, *101*, 7633-7642.
- (22) Likholyot, A.; Lemke, K. H.; Hovey, J. K.; Seward, T. M. *Geochim. Cosmochim. Acta* **2007**, *71*, 2436-2447.
- (23) Lungdren, J.-O.; Olovsson, I. In *The Hydrogen Bond: II. Structure and Spectroscopy*; Schuster, P.; Zundel, G.; Sandorfy, C., Eds.; North-Holland: Amsterdam, 1976; Chap. 10.

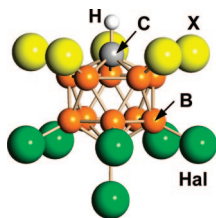


Figure 1. Conjugate base carborane anions of the type $CHB_{11}X_5Hal_6^-$ used in this work ($X/Hal = H/Br, Cl/Cl, I/I$).

Given these considerations, as well as the importance of the hydrated proton in acid catalysis, fuel cell electrolytes, and acid/base chemistry in general, we are focusing on the nature of the hydrated proton in organic solvents, where studies are few. Just as in the gas phase, water molecules can be controlled and sequentially attached to the proton, forming $H(H_2O)_n^+$ clusters. The ease of formation, structure, and composition of these cations depend strongly on the basicity of the solvent and the basicity of the anion, i.e., the strength of the conjugate acid. In weakly basic solvents like CH_2Cl_2 , acids such as HCl are hydrated mainly without proton transfer to H_2O molecules.²⁴ Simple H-bonded solvates of the type $HA \cdot (H_2O)_n$ prevail rather than ionized $H(H_2O)_n^+$ clusters. With solvents of higher basicity such as tributylphosphate (TBP), whose basicity is close to that of water, proton transfer to H_2O becomes possible but is accompanied by waterless TBP \cdot HA monosolvates.²⁵ Stronger acids such as perchloric and triflic acids certainly protonate water in weakly basic solvents, but the solubilities of the ionized species are low and often insufficient to study their full hydration by IR. Thus, only the mono- and dihydrates of triflic acid, $H_3O^+OTf^-$ and $H_5O_2^+OTf^-$, have been studied in dichloroethane.²⁶ With increasing solvent basicity, the solubilities of strong acids increase. In TBP for example, $HClO_4$ and $HFeCl_4$ form a set of $H(H_2O)_n^+$ clusters with step-by-step increasing n up to aggregates with high n that are like reverse nanomicelles.^{27,28} The protons are located in the water core of these micelles near the boundary with the TBP solvation shell in the form of tetrasolvated $H_5O_2^+$ ions, $[H_5O_2^+ \cdot 2H_2O \cdot 2TBP]$. The counterions are weakly ion-paired to the water micelle in the case of ClO_4^- but remote and non-interacting in the case of the more weakly basic $FeCl_4^-$ anion. These observations highlight the need for a strong acid whose $H(H_2O)_n^+$ salts are soluble in low-basicity solvents and whose anion will have minimal influence on the structures of the $H(H_2O)_n^+$ cations.

Suitable acids have recently become available in carborane superacids, $H(CHB_{11}R_5X_6)$ ($R = H, Cl, Br, I; X = Cl, Br, I$; see Figure 1).²⁹ They are presently the strongest known pure acids,^{30,31} and their conjugate base anions impart good solubility to salts in low-basicity solvents. Their large, nonpolarizable anions are expected to have the weakest influence on the structure of the cations, possibly leading to $H(H_2O)_n^+$ cations

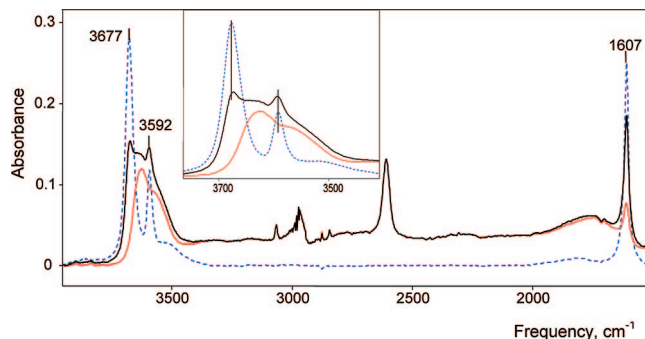


Figure 2. IR spectrum of $H(H_2O)_n^+ \{H_3Br_6^-\}$ in DCE solution with $N = 3.7$ after sequential subtraction of dry DCE and hexamethylbenzene (black) and then free dissolved water, resulting in the final spectrum (red). For reference, the spectrum of 0.1 M water in DCE (after subtracting DCE) is shown in dashed blue.

that reflect those in the gas phase. We have previously used carborane acids to establish the nature of the H_3O^+ and $H_5O_2^+$ ions under controlled conditions of minimal water content.^{5,7} We now apply these methods to the more normal laboratory conditions of wet organic solvents, where higher hydrates prevail. Benzene and dichloroethane are chosen because they are common solvents for synthetic chemistry.

Experimental Section

Carborane acids $H(CHB_{11}H_5Br_6)$, $H(CHB_{11}Cl_{11})$, and $H(CHB_{11}I_{11})$ (abbreviated $H\{H_5Br_6\}$, $H\{Cl_{11}\}$, and $H\{I_{11}\}$, respectively) and their arenium ion salts were prepared as previously described.³⁰ Chlorinated cobalt(III) dicarbollide, $Co(C_2B_9H_8Cl_3)_2^-$ (abbreviated $\{CCD^-\}$; 90% in H-form and 10% in Na-form), with an analysis of 9.35% Co and 29.05% Cl, was received from KatChem (Czech Republic) and converted into 100% H-form $H\{CCD\}$ by shaking a dichloroethane (DCE) solution with a 3 M H_2SO_4 aqueous solution for 5 min and retaining the DCE layer. Benzene and DCE were purified and dried according to literature methods.³² $H^+(H_2O)_n \{H_3Br_6\}$ solutions in DCE were prepared by mixing calculated volumes of dry DCE, water-saturated DCE containing 0.1 M H_2O , and 0.025 M $C_6Me_6H^+ \{H_3Br_6^-\}$ or $C_6H_7^+ \{H_3Br_6^-\}$ solutions in DCE to obtain solutions with constant acid concentration C_{HCarb} and defined water concentration $C_{H_2O}^0$. For solutions with $H_2O/acid$ molar ratio equal to 2–3, C_{HCarb} was 0.015 M. For $H_2O/acid > 3$, C_{HCarb} was 0.01 M. Solutions with the largest fixed $H_2O/acid$ molar ratios were obtained by dissolving weighed portions of $C_6H_7^+ \{H_3Br_6^-\}$ in DCE containing 0.1 M H_2O . Benzene solutions of $H^+(H_2O)_n \{H_3Br_6^-\}$ and $H^+(H_2O)_n \{Cl_{11}^-\}$ were prepared in a manner similar to the preparation of the DCE solutions, using water-saturated benzene (0.2 M) and weighed quantities of mesitylenium or hexamethylbenzenium salts dissolved in water-saturated benzene. The final benzene solutions contained 0.004 M $H^+(H_2O)_n \{H_3Br_6\}$ or 0.005 M $H^+(H_2O)_n \{Cl_{11}\}$. The spectrum of free hexamethylbenzene or mesitylene (formed in solution) was digitally subtracted. Water-saturated $H^+(H_2O)_n Carb^-$ solutions, with $Carb^- = \{H_3Br_6^-\}, \{Cl_{11}^-\}, \{I_{11}^-\}$, and $\{CCD^-\}$, were obtained by extraction of the acids from aqueous solutions. The concentrations of all acids were measured by the intensity of the anion absorption bands in IR spectra.

The IR spectra of these solutions consist of overlapping spectra of the following components: (i) solvent, (ii) water dissolved in the solvent, and (iii) hydrated acid, $H(H_2O)_n^+ Carb^-$. To isolate the spectrum of a particular $H^+(H_2O)_n Carb^-$ species, the spectra of the solvent and dissolved water were successively subtracted from the initial spectrum. Figure 2 shows a typical example of this

(24) Pankov, A. A.; Borovkov, V. Yu.; Kazanski, V. B. *J. Appl. Spectrosc. (Russian)* **1982**, *37*, 824–825.

(25) Stoyanov, E. S.; Mikhailov, V. A.; Chekmarev, A. M. *Zr. Neorg. Khim. (Russian)* **1990**, *35*, 1442–1450.

(26) Stoyanov, E. S.; Kim, K.-C.; Reed, C. A. *J. Phys. Chem. A* **2004**, *108*, 9310–9315.

(27) Stoyanov, E. S. *J. Chem. Soc., Faraday Trans.* **1997**, *93*, 4165–4175.

(28) Stoyanov, E. S. *J. Chem. Soc., Faraday Trans.* **1998**, *94*, 2803–2812.

(29) Reed, C. A. *Chem. Commun.* **2005**, 1669–1677.

(30) Juhasz, M.; Hoffmann, S.; Stoyanov, E.; Kim, K.-C.; Reed, C. A. *Angew. Chem., Int. Ed.* **2004**, *43*, 5352–5355.

(31) Stoyanov, E. S.; Kim, K.-C.; Reed, C. A. *J. Am. Chem. Soc.* **2006**, *128*, 8500–8508.

(32) Armarego, W. L. F.; Perrin, D. D. *Purification of Laboratory Chemicals*, 4th ed.; Educational and Professional Publishing Ltd.: Oxford, 1996.

procedure. Subtraction of the dissolved water using spectra of 0.1 M water-saturated DCE or 0.2 M water-saturated benzene with a scaling factor f_i allowed determination of the concentration of “free” water dissolved in the solutions under study: $C_{\text{H}_2\text{O}}^{\text{free}} = f_i C^{\text{sat}}$, where $C^{\text{sat}} = 0.1$ and 0.2 M for DCE and benzene, respectively. The concentration of water involved in the $\text{H}(\text{H}_2\text{O})_n^+$ cation is determined from the difference $C_{\text{H}_2\text{O}}^{\text{cat}} = C_{\text{H}_2\text{O}}^{\text{O}} - C_{\text{H}_2\text{O}}^{\text{free}}$, where $C_{\text{H}_2\text{O}}^{\text{O}}$ is the total water concentration, known from the conditions of preparation. The ratio $N = C_{\text{H}_2\text{O}}^{\text{cat}}/C_{\text{Hcarb}}$ gives the average stoichiometry of $\text{H}(\text{H}_2\text{O})_n^+$ cations formed in solution. This method of spectral subtraction to determine the concentration of water (or methanol)³³ bound with H^+ and the average N stoichiometry of the formed $\text{H}^+ \cdot \text{L}_N$ cations has been previously described in detail.^{27,28,34}

The water-saturated DCE solutions of $\text{H}(\text{H}_2\text{O})_n^+ \{\text{I}_{11}^-\}$ and $\text{H}(\text{H}_2\text{O})_n^+ \{\text{CCD}^-\}$ acids were prepared by extraction from water solution of their $\text{Cs}\{\text{I}_{11}\}$ or $\text{H}/\text{Na}\{\text{CCD}\}$ salts containing 2–4 M H_2SO_4 . The separated organic phase was washed four or five times with 1–2 M H_2SO_4 and then with distilled water. The molar concentrations of the acids were determined from the intensity of IR absorption of the $\{\text{I}_{11}^-\}$ and $\{\text{CCD}^-\}$ anions compared to standard DCE solutions of $(\text{Oct})_3\text{NH}^+\{\text{I}_{11}^-\}$ or $(\text{Oct})_3\text{NH}^+\{\text{CCD}^-\}$. The total water concentration was determined using ^1H NMR. The initial DCE solvent was made 0.2 M in chloroform as an internal standard. In the NMR spectra of water-saturated DCE solutions, the signal integrations of chloroform (at 7.26 ppm) and water (at 1.49 ppm) give the ratio 1.00:1.03, in good agreement with the known water content of 0.1 M.³⁵ In the spectra of $\text{H}(\text{H}_2\text{O})_n^+ \{\text{I}_{11}^-\}$ and $\text{H}(\text{H}_2\text{O})_n^+ \{\text{CCD}^-\}$, the ratio of these signals allowed determination of the total water concentration, $C_{\text{H}_2\text{O}}^{\text{O}}$, and the molar ratio $N = (C_{\text{H}_2\text{O}}^{\text{O}} - 0.1)C_{\text{Hcarb}}$.

With the exception of water-saturated solvents, all solutions were prepared in a Vacuum Atmospheres Corp. glovebox under nitrogen (O_2 , $\text{H}_2\text{O} < 0.5$ ppm). IR spectra in the 4000–450 cm^{-1} range were run on a Shimadzu-8300 FT-IR spectrometer housed inside a glovebox. A cell with Si windows having 0.036 mm separation at the beam transmission point was used. To avoid interference effects, the cell configuration was wedge-shaped. IR data were manipulated using GRAMMS software. NMR spectra were run on a Varian INOVA 400 spectrometer.

X-ray-quality crystals of $[\text{H}_7\text{O}_3^+][\text{CHB}_{11}\text{Cl}_{11}]$ were grown from *o*-dichlorobenzene under conditions of slow solvent evaporation at low pressure. Crystals of $[\text{H}(\text{CH}_3\text{OH})_3^+][\text{CHB}_{11}\text{Cl}_{11}]$ were grown from benzene solution with a 1:3 MeOH/ $[\text{Cl}_{11}]$ mole ratio.³³ Crystals of $[\text{H}_9\text{O}_4^+][\text{CHB}_{11}\text{Cl}_{11}]$ were grown from water-saturated $\text{H}[\text{CHB}_{11}\text{Cl}_{11}]$ solution in a desiccator over CaCl_2 . The crystallographic data for these salts are available in the Supporting Information or can be obtained free of charge from The Cambridge Crystallographic Data Centre at www.ccdc.cam.ac.uk/data_request/cif (CCDC 687306, 687307, and 687308).

Results and Discussion

IR spectra of benzene and DCE solutions of carborane acids with different water/acid mole ratios $N = \text{H}_2\text{O}/\text{H}(\text{carborane})$ change regularly with increasing N , indicating sequential of hydration of H^+ . In addition, water molecules may be involved with solvation of the carborane anions. In order to examine this possibility, we studied dichloroethane extracts of cesium carborane salts from water solutions. In addition to the bands from the carborane anions and dissolved water, IR spectra of these extracts developed two new narrow OH stretching bands, ν_{as} at 3655 and ν_{s} at 3578 cm^{-1} , arising from H_2O molecules with

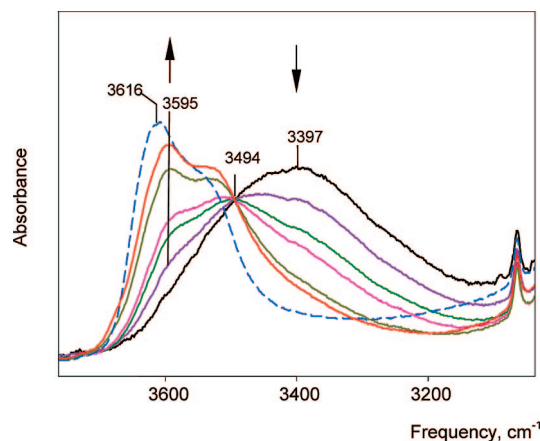


Figure 3. IR spectra of $\text{H}(\text{H}_2\text{O})_n^+$ cations with $n = 2.0, 2.16, 2.30, 2.45, 2.75, 2.85,$ and 3.06 in DCE solutions. The initial spectrum (black) belongs to H_5O_2^+ . The red spectrum belongs to the $\alpha\text{-H}_7\text{O}_3^+$ isomer and the final (blue dashed) spectrum to the $\beta\text{-H}_7\text{O}_3^+$ isomer.

free OH groups. Since these frequencies are independent of the nature of the carborane anion and are red-shifted compared to those for dissolved monomeric water molecules in DCE (3675 and 3591 cm^{-1} , respectively), they are assigned to H_2O molecules bound to the Cs^+ cation via the O atom. Thus, there are no water molecules involved with hydrating the carborane anions. Taking into account that the νOH frequencies of the $\text{H}(\text{H}_2\text{O})_n^+$ cations discussed below are also independent of the nature of carborane anion, we can conclude that the OH groups of the cations are not H-bonded with counterion. This is consistent with our earlier studies on the $\text{H}_5\text{O}_2^+ \cdot 4\text{Solv}$ cations⁷ where, although there is good evidence for ion pairing, H-bonding of the cation occurs only with solvent molecules. Thus, solvent-separated ion pairs of the type $[\text{H}^+(\text{H}_2\text{O})_n \cdot m\text{Solv}]\text{Carb}^-$ are formulated in the present work.

DCE Solutions. IR spectra of $\text{H}(\text{H}_2\text{O})_n^+ \{\text{H}_5\text{Br}_6^-\}$ solutions with water/acid mole ratios $N \geq 2$ have been studied. The spectrum of the solution with $N = 2$ belongs to the $\text{H}_5\text{O}_2^+ \cdot 4\text{DCE}$ cation.⁷ With gradually increasing N to 3, the intensity of the H_5O_2^+ spectrum decreases and disappears. At the same time, the spectrum of the H_7O_3^+ cation appears and reaches a maximum at $N = 3$. As shown in Figure 3, there is an isosbestic point at 3494 cm^{-1} up to $N = 2.9$, confirming that, in this range, only two cations, H_5O_2^+ and H_7O_3^+ , are formed (i.e., $N = n$). As $N = 3$ is approached, there is a peculiar step change in the H_7O_3^+ spectrum (Figure 3). This change is consistently reproducible and indicates the existence of two forms of the H_7O_3^+ cation: the α isomer at $N < 3$ and the β isomer at $N > 3$. Their individual spectra are shown in Figure 4 and, as discussed in more detail below, are ascribed to different degrees of ion pairing. With further increase of N from 3 to 5.2, the spectrum of $\beta\text{-H}_7\text{O}_3^+$ is transformed into that for the more highly hydrated $\text{H}(\text{H}_2\text{O})_n^+$ cations with isosbestic points at 3542 and 3467 cm^{-1} (Figure 5). This means either that H_7O_3^+ is transformed into a single $\text{H}(\text{H}_2\text{O})_n^+$ cation with constant n , which seems improbable, or that a set of spectroscopically indistinguishable compounds with variable $n \geq 4$ are formed, which will need a specific explanation.

Proton hydrates can be followed as a function of N via the change in frequency of $\nu_{\text{as}}\text{H}_2\text{O}$ from the terminal H_2O molecules, i.e., the “free” OH groups that are H-bonded to solvent. The $\nu_{\text{as}}\text{H}_2\text{O}$ band is chosen over $\nu_{\text{s}}\text{H}_2\text{O}$ for this analysis because it does not overlap with bands from other types of vibrations. As

(33) Stoyanov, E. S.; Stoyanova, I. V.; Reed, C. A. *Chem. Eur. J.* **2008**, *14*, 3596–3604.

(34) Stoyanov, E. S. *Phys. Chem. Chem. Phys.* **1999**, *1*, 2961–2966.

(35) (a) Staverman, A. J. *Recl. Trav. Chim. Pays-Bas* **1941**, *60*, 836–841. (b) Barr, R. S.; Newsham, D. M. T. *Fluid Phase Equilib.* **1987**, *35*, 189–205.

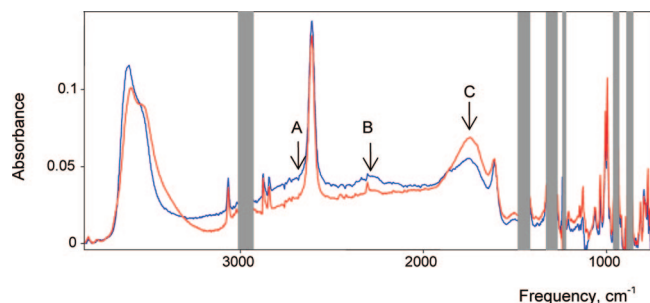


Figure 4. IR spectra of $H_7O_3^+$ isomers α (red) and β (blue).

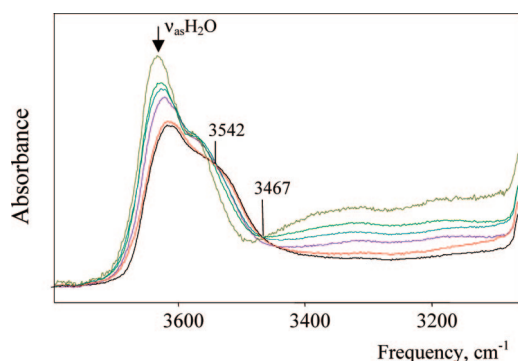


Figure 5. IR spectra of $H(H_2O)_n^+$ cations with $n = 3.02\text{--}5.22$.

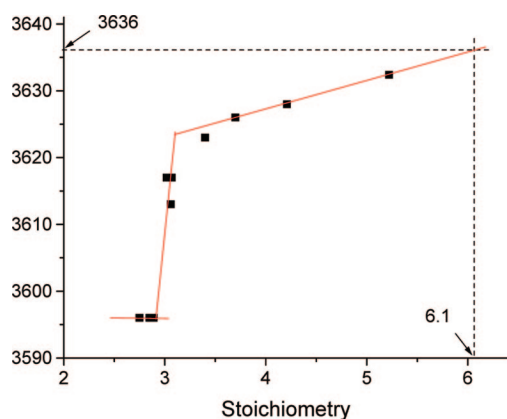
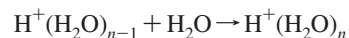


Figure 6. Dependence of $\nu_{as}H_2O$ on the stoichiometry n of $H(H_2O)_n^+$.

shown in Figure 6, for $N = 2\text{--}3$, the $\nu_{as}H_2O$ frequency of $\alpha\text{-}H_7O_3^+$ is constant. At $N \approx 3$, the $\alpha\text{-}\beta$ isomerism of $H_7O_3^+$ takes place, and $\nu_{as}H_2O$ jumps steeply. In the range $N > 3$, $\nu_{as}H_2O$ bands of $\beta\text{-}H_7O_3^+$ and higher $H(H_2O)_n^+$ hydrates are strongly overlapped, and their joint maximum weakly increases in frequency as cations with $n > 3$ are formed. The procedures necessary to obtain samples of known water concentration (see Experimental Section) do not allow the total water concentration to exceed that of water-saturated DCE (0.1 M), and the maximum N value we can study is 5.2. On the other hand, a DCE extract from aqueous $H\{H_3Br_6\}$ has a higher total concentration of water, and the $\nu_{as}H_2O$ frequency is $3636 \pm 1 \text{ cm}^{-1}$. Extrapolation using the Figure 6 dependence indicates that this frequency corresponds on average to the $H(H_2O)_6^+$ cation.

If successive $H(H_2O)_n^+$ cations have strongly differing stability constants K_n , then the dependence of the free dissolved water concentration $C_{H_2O}^{free}$ on n should be stepped since, in accordance with equilibria

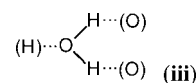


the equilibrium constant $K_n = C_n/C_{n-1}C_{H_2O}^{free}$ includes, in addition to C_n and C_{n-1} , the concentrations of $H(H_2O)_n^+$ and $H(H_2O)_{n-1}^+$ cations, respectively, the concentration of free dissolved water, $C_{H_2O}^{free}$. However, as shown in Figure 7, the dependence of $C_{H_2O}^{free}$ on n shows only one step at $n = 3$, when formation of $H_7O_3^+$ cation is complete and a detectable concentration of free dissolved water appears. With further increasing n , the dependence increases steeply and linearly, indicating that the K_n constants for cations with $n \geq 4$ are low and do not differ significantly. Extrapolation to water-saturated DCE ($C_{H_2O}^{free} = 0.1 \text{ M}$) results in $n = 6$, confirming that the highest formed proton hydrate is the $H(H_2O)_6^+$ ion. The dependence of $C_{H_2O}^{free}$ on n allows the determination of K_n values for cations with $n \geq 4$. For equal concentrations of $H^+(H_2O)_n$ and $H^+(H_2O)_{n+1}$ cations, $K_n = 1/C_{H_2O}^{free}$, where $C_{H_2O}^{free}$ is the free water concentration for solutions with $C_n = C_{n-1}$. From $C_{H_2O}^{free} = f(n)$, one can determine that $C_{H_2O}^{free} = 0.0385$, 0.0628 , and 0.0876 M respectively for solutions with $N = 3.5$, 4.5 , and 5.5 . Then, $K_4 = 26.0$, $K_5 = 15.9$, and $K_6 = 11.4$. The K_3 value, for the formation of the $H_7O_3^+$ cation, cannot be determined since the $C_{H_2O}^{free}$ concentration required for calculation is below the threshold of IR detectability.

For all $H(H_2O)_n^+$ cations with $n \geq 3$, the frequency of the δH_2O terminal water bending vibration is practically the same, 1608 cm^{-1} . Its intensity (I_{1608}) increases linearly with increasing $H_7O_3^+$ cation concentration in solutions as N increases from 2 to 3 and extrapolates to zero at $N = 2$ (Figure 8). This confirms a peculiarity established earlier, namely that, in the IR spectrum of the $H_5O_2^+$ cation, the δH_2O band is not observed.⁷ At $N \approx 3$, the I_{1608} dependence on N changes slope and then continues to grow with increasing n , in line with the increasing number of terminal water molecules in $H(H_2O)_n^+$ cations. They can contain two types of terminal H_2O : type (i), with both OH groups free, or type (ii), with one free and the other H-bonded.



Their δH_2O frequencies coincide because the addition of a single H-bond in (ii) has a minimal effect on the force constant of this vibration. On the other hand, when both O–H groups are H-bonded to additional water molecules, as in coordination type (iii), the δH_2O frequency is detectably higher.



In summary, IR spectra of DCE solutions show that only the $H_5O_2^+$ and $H_7O_3^+$ cations have specific identities. $H(H_2O)_n^+$ cations with $n = 4\text{--}6$ develop as a single family of compounds with spectroscopic properties sufficiently similar that it is impossible to detect their successive formation. They differ only slightly in the bands arising from their terminal water molecules.

Benzene Solutions. The IR spectra of $H(H_2O)_n^+$ cations in benzene solution are quite similar to those for DCE and are essentially independent of the nature of the counterion, $\{Cl_{11}^-\}$ or $\{Me_5Br_6^-\}$. Therefore, we will discuss the spectra of solutions of the $H\{Cl_{11}\}$ acid, whose hydrates are more soluble in benzene.

The spectrum of the cation formed in solution with $N = 2$ belongs to $H_5O_2^+$.⁷ With N increasing to 3, the intensity of the

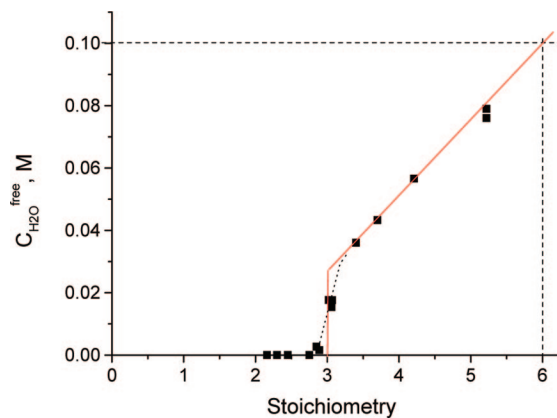


Figure 7. Dependence of the concentration of free dissolved water on stoichiometry of the $\text{H}(\text{H}_2\text{O})_n^+$ cations formed.

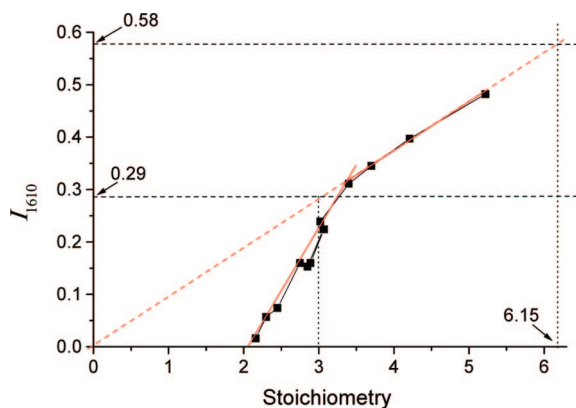


Figure 8. Dependence of the $\delta\text{H}_2\text{O}$ band intensity on the stoichiometry of the $\text{H}(\text{H}_2\text{O})_n^+$ cations.

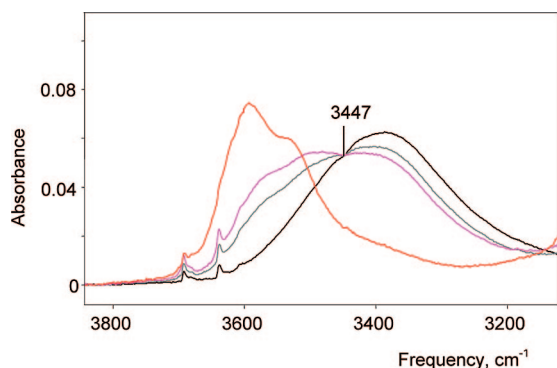


Figure 9. IR spectra of $\text{H}(\text{H}_2\text{O})_n^+$ cations with $n = 1.99, 2.35, 2.55,$ and 2.91 in benzene solution in the frequency range of νOH of the terminal OH groups. The initial spectrum (black) belongs to H_5O_2^+ . The red spectrum belongs to the $\beta\text{-H}_7\text{O}_3^+$ isomer.

H_5O_2^+ spectrum decreases as the spectrum of the H_7O_3^+ cation increases, with an isosbestic point at 3447 cm^{-1} (Figure 9). However, in the range of $N = 2.6\text{--}2.9$, the spectrum of the H_7O_3^+ cation changes rapidly such that, at $N = 3$, the spectrum does not cross the isosbestic point. Just as in DCE solution, the H_7O_3^+ cation must exist in two isomeric forms in benzene solution: α ($N = 2\text{--}2.6$) and β ($N \geq 2.9$). Their spectra are given in Figure 10.

With increasing N from 3 to 4, the spectra change, with a new isosbestic point at 3544 cm^{-1} indicating transformation of the H_7O_3^+ cation into $\text{H}(\text{H}_2\text{O})_n^+$ (Figure 11). The spectra with $N > 4$ do not cross exactly at 3544 cm^{-1} , indicating that the

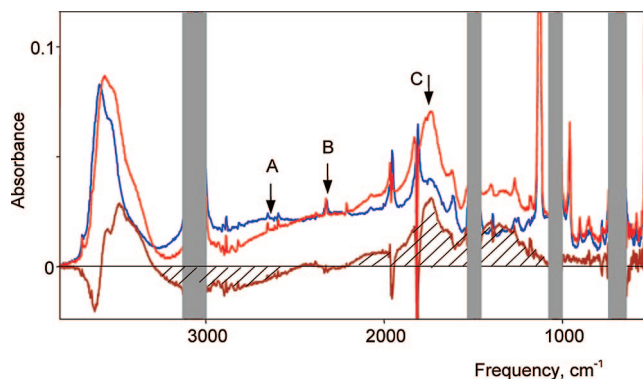


Figure 10. IR spectra of α (red) and β (blue) isomers of the H_7O_3^+ ion, equalized to unit intensity of the $\{\text{Cl}_{11}\}^-$ anion, and the difference spectrum (brown) with hatching showing positive and negative intensity.

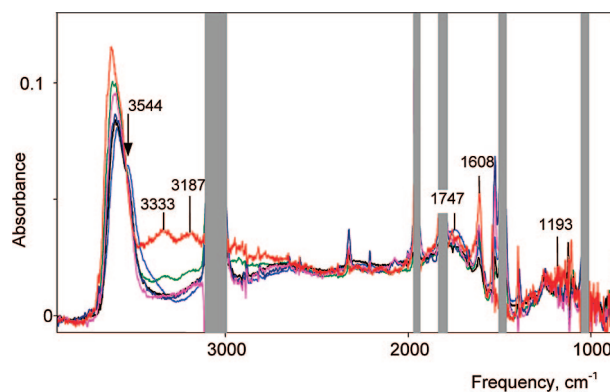
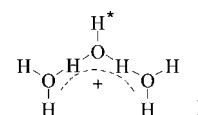


Figure 11. Spectra of $\text{H}^+(\text{H}_2\text{O})_n\{\text{Cl}_{11}\}$ in benzene solutions with $N = 3.2, 3.42, 3.46, 3.91,$ and 4.52 . The red spectrum is close to water-saturated with undetermined N . The bands from $\{\text{Cl}_{11}\}^-$ anion were subtracted using the spectrum of $(\text{Oct})_3\text{NH}\{\text{Cl}_{11}\}$ solution in benzene.

$\text{H}(\text{H}_2\text{O})_4^+$ cation may differ slightly more from cations with $n \geq 5$ in benzene compared to DCE.

Spectra and Structures of the $\text{H}(\text{H}_2\text{O})_n^+$ Cations. H_7O_3^+ . IR spectra of the α and β isomers of the H_7O_3^+ cation are both in agreement with the symmetrical cation structure **I**.



They show two types of OH stretching vibrations from terminal OH groups: first, $\nu_s\text{H}_2\text{O}$ and $\nu_{as}\text{H}_2\text{O}$ from the two equivalent H_2O molecules and second, a lower frequency νOH band from the group labeled OH^* in **I**. The deconvolution is shown in Figure 12, and the data are listed in Table 1. The $\delta\text{H}_2\text{O}$ bend is at 1608 cm^{-1} . Vibrations from the conjugated $(\text{O}\cdots\text{H}-\text{O}-\text{H}\cdots\text{O})^+$ group develop as a continuous broad absorption in the range $1400\text{--}3100\text{ cm}^{-1}$ (Figures 4 and 10) with a particular shape (discussed below). The OH stretching frequencies of the terminal OH groups of the α isomer are somewhat red-shifted compared with those for the β isomer, and the band intensity is slightly higher (Figures 4, 10, and 12). This means that the α isomer experiences a somewhat stronger interaction with its environment. It is likely that $\alpha\text{-H}_7\text{O}_3^+$ forms mixed-ion associates of the type $(\text{H}_7\text{O}_3^+)_x(\text{H}_5\text{O}_2^+)_y\text{Carb}^{-(x+y)}$ since the α isomer exists only in the presence of H_5O_2^+ when $N < 3$. The destruction of these mixed associates as N approaches 3 can be understood in terms of the disappearance

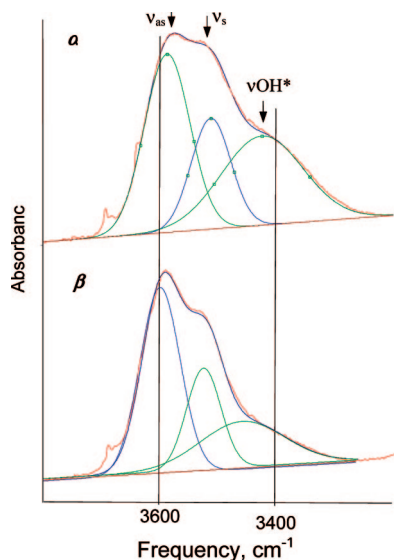


Figure 12. Deconvolution of the IR spectra of the α and β isomers of $H_7O_3^+$ in benzene in the frequency range of the terminal OH groups.

Table 1. Frequencies of Terminal OH Stretching Vibrations in $H_7O_3^+$

solvent	band	frequency		$\Delta\nu(\beta - \alpha)$
		α isomer	β isomer	
DCE	$\nu_{as}H_2O$	3595	3612	17
	ν_sH_2O	3520	3535	14
	νOH^*	<i>a</i>	<i>a</i>	<i>a</i>
Benzene	$\nu_{as}H_2O$	3576	3597	21
	ν_sH_2O	3501	3523	21
	νOH^*	3416	3458	42

^a Cannot be determined with reliable accuracy.

of the $H_5O_2^+$ ion, resulting in the formation of the β isomer. Related associates were found in reverse nanomicelles formed in wet TBP solutions of $HFeCl_4$ and HCl .²⁸ They have a specific $HFeCl_4/HCl$ mole ratio and are destroyed when this molar ratio is not supplied.

The distinctive continuous broad absorption (*cba*) in the spectrum of $H_7O_3^+$ in the 1400–3100 cm^{-1} frequency range, which notably is absent in the spectrum of the $H_5O_2^+$ cation,⁷ derives from the $(O\cdots H-O-H\cdots O)^+$ group vibrations. A similar feature is observed in the spectra of all other compounds containing the $O-H\cdots O$ group, as long as the condition of $O\cdots O$ distance in the range 2.51–2.60 Å is fulfilled. As shown in Table 2, this group of compounds includes dimers of dialkylphosphoric and dialkylphosphinic acids, the salts of carboxylic acids with organic basics, and a variety of other acid salts. The IR spectra of compounds containing a conjugated (biprotonic) group of the $(X\cdots H-O-H\cdots X)^+$ type with $X =$ heteroatom, whose stretching and bending vibrations are strongly coupling, nevertheless develop the same *cba*.^{48,49} The shape of the *cba* is quite specific, having so-called A (~ 2600 – 2800 cm^{-1}), B (~ 2200 cm^{-1}), and C (1700 – 1800 cm^{-1}) structure.⁵⁰

There are different points of views on the interpretation of the A, B, C structure of the *cba* band,⁵¹ but Fermi resonance between the νOH stretch and the overtones of low-frequency vibrations of the $O-H\cdots O$ group, namely with the first overtones of the in-plane $\delta(OHO)$ (A and B bands) and out-of-plane $\gamma(OHO)$ (C band) vibrations, is gaining wide accep-

tance.^{36–38,52,53} The Fermi resonance nature of the A, B, and C bands and the correct assignments of the $\delta(OHO)$ and $\gamma(OHO)$ bands have been rigorously confirmed on the basis of polarization data in the IR and Raman bands in the spectra of acid sulfates, phosphates, and selenates of potassium and cesium at 300 and 20 K.^{39,41,42}

Since the *cba* represents a very broad OH stretching band and its shape is distorted by Fermi resonance, νOH is determined as the center of gravity of *cba* absorption.^{37,38} The *cba* does not significantly depend on the energy/enthalpy of the H-bonding, the temperature (80–550 K), or the state of matter.⁴⁵ However, the center of gravity (i.e., νOH) depends on $O\cdots O$ distance. With $O\cdots O$ decreasing to 2.41–2.42 Å as in the $H_5O_2^+$ cation^{3,4} or to 2.39 Å as in proton disolvates $L-H^+-L$ (with $L =$ strong base),⁵⁴ νOH decreases in frequency. As $O\cdots O$ decreases, bands A and B decrease in intensity and disappear when $H_7O_3^+$ becomes $H_5O_2^+$. Band C is retained, and new bands in the low-frequency 800–1200 cm^{-1} region appear in the spectrum of $H_5O_2^+$.⁷

In crystalline $H_7O_3^+\{Cl_{11}\}$, the $H_7O_3^+$ cation is asymmetric with one $O\cdots O$ distance longer, 2.518(2) Å, and the other shorter, 2.439(2) Å, reflecting the asymmetrical environment of $\{Cl_{11}^-\}$ anions. Such asymmetry is common for $H_7O_3^+$ cations in the crystalline state; for example, $[H_7O_3\cdot(15\text{-crown-5})][AuCl_4]^{55}$ has 2.536(7) and 2.423(7) Å $O\cdots O$ distances. The shorter distance in the $H_5O_2^+$ cation (2.40–2.42 Å)^{3,4,7} suggests formulation of these salts as $H_5O_2^+$ monohydrates, $H_5O_2^+\cdot H_2O$. However, the IR spectrum of the distorted $H_7O_3^+$ cation in crystalline $H_7O_3^+\{Cl_{11}\}$ shows a strong *cba* with A, B, C structure, not seen for the $H_5O_2^+$ cation, arising from the $O\cdots H-O-H\cdots O$ chromophore (Figure 13). Thus, it has a separate identity. Since its IR spectrum differs considerably from

- (36) Odínokov, S. E.; Iogansen, A. V. *Spectrochim. Acta* **1972**, *28A*, 2343–2350.
- (37) Glazunov, V. P.; Mashkovskii, A. A.; Odínokov, S. E. *Zh. Prikl. Spektrosk.* **1975**, *22*, 696–702.
- (38) Mashkovskii, A. A.; Glazunov, V. P.; Odínokov, S. E. *Zh. Prikl. Spektrosk.* **1974**, *20*, 852–856.
- (39) Baran, J.; Lis, T.; Ratajczak, H. *J. Mol. Struct.* **1989**, *195*, 159–174.
- (40) Bertoluzza, A.; Battaglia, M. A.; Bonora, S.; Monti, H. *J. Mol. Struct.* **1985**, *127*, 35–45.
- (41) Baran, J. *J. Mol. Struct.* **1987**, *162*, 211–228.
- (42) Baran, J. *J. Mol. Struct.* **1987**, *162*, 229–245.
- (43) Detoni, S.; Hadzi, D. *J. Chem. Phys.* **1956**, *53*, 760–764.
- (44) Stoyanov, E. S.; Popov, V. M.; Mikhailov, V. A. *Zh. Prikl. Spektrosk.* **1984**, *40*, 77–84.
- (45) Asfin, R. A.; Denisov, G. S.; Tokhadze, K. G. *J. Mol. Struct.* **2002**, *608*, 161–168.
- (46) Solka, J. L.; Reis, A. H.; Mason, G. W.; Lewey, S. M.; Peppard, D. F. *J. Inorg. Nucl. Chem.* **1978**, *40*, 663–668.
- (47) Gebert, E.; Reis, A. H.; Peterson, S. W.; Katzin, L. I.; Mason, G. W.; Peppard, D. F. *J. Inorg. Nucl. Chem.* **1981**, *43*, 1451–1464.
- (48) Brzezinski, B.; Maciejewska, H.; Zundel, G.; Kramer, R. *J. Phys. Chem.* **1990**, *94*, 528–531.
- (49) Brzezinski, B.; Maciejewska, H.; Zundel, G. *J. Phys. Chem.* **1990**, *94*, 6983–6986.
- (50) Hadzi, D.; Kobilarov, N. *J. Chem. Soc. A* **1966**, 439–445.
- (51) Hofacker, G. L.; Marechal, Y.; Ratner, M. A. In *The Hydrogen Bond*; Shuster, P.; Zundel, G.; Sandorfy, C., Eds.; North-Holland: Amsterdam, 1976; Vol. 1, pp 683–766.
- (52) Claydon, M. F.; Sheppard, N. *J. Chem. Soc. D* **1969**, 1431–1433.
- (53) Bratos, S.; Lascombe, J.; Novak, A. In *Molecular Interactions*; Ratajczak, H., Orvill-Thomas, W. J., Eds.; Wiley: Chichester, 1980; pp301–346.
- (54) Stasko, D.; Hoffmann, S. P.; Kim, K.-Ch.; Fackler, N. L. P.; Larsen, A. S.; Drovetskaya, T.; Tham, F. S.; Reed, C. A.; Rickard, C. E. F.; Boyd, P. D. W.; Stoyanov, E. S. *J. Am. Chem. Soc.* **2002**, *124*, 13869–13876.
- (55) Calleja, M.; Johnson, K.; Belcher, W. J.; Steed, J. W. *Inorg. Chem.* **2001**, *40*, 4978–4985.

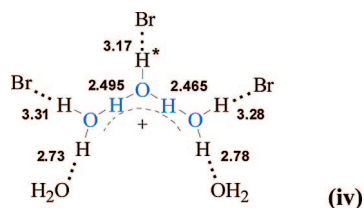
Table 2. Frequencies of O–H···O Groups for Selected Compounds That Develop the Continuous Broad IR Absorption with A, B, and C Contours

type of O–H···O group	compound	method	stretching vibration			bending vibration ^a		$R_{O\dots O}$, Å	ref
			A	B	C	$\delta(\text{OHO})$	$\gamma(\text{OHO})$		
(C)O–H···O(X)	H-complexes of carboxylic acids	IR	2800	2500	1900	1200–1600	900–1100		36–38
(O ₃ P)O–H···O(PO ₃)	K ₂ HPO ₄ ·3H ₂ O	IR	2700	2330 2265	1670 1700	1220	800	2.578	39
(O ₃ P)O–H···O(PO ₃)	Ca(H ₂ PO ₄) ₂ ·H ₂ O	IR	2920	2375	1700	*	*	2.596	40
(S)O–H···O(S)	CsHSO ₄	IR, Raman	2850	2500	1680	1252	884	2.572	41
(Se)O–H···O(Se)	CsHSeO ₄	IR, Raman	2840	2415	1600	1258	805	2.603	42
(Se)O–H···O(Se)	C ₆ H ₅ SeOOH	IR	2740	2270	1650	*	*	2.52	43
(P)O–H···O(P)	dialkylphosphoric and dialkylphosphinic acids	IR ^{44,45}	2600–2800	2200–2400	1610–1700	*	*	2.53 ⁴⁶ 2.51 ⁴⁷	

^a Asterisk indicates “no data”.

that in solution (Figure 13), we should compare it to that in a more symmetrical crystalline environment.

The structure reported to have the most symmetrical H₇O₃⁺ cation is found in [H₇O₃⁺][H₉O₄⁺]⁺Br₂[−]·H₂O, where the O···O distances are 2.47(1) and 2.50(1) Å (average 2.481 Å).⁵⁶ The symmetry arises from a nearly symmetrical anion/hydrate field, as shown in (iv).



The proton labeled H* is more tightly H-bonded to bromide than those from the terminal water molecules, reflecting its closer proximity to the positive charge. The interaction with two water solvate molecules is weak. Unfortunately, because of the presence of H₉O₄⁺ (and H₂O) in these crystals, they are not suitable for IR investigation of the H₇O₃⁺ ion. Lacking good hydrates for structure/spectra correlation, we turn to the methanol analogue of the H₃O₃⁺ ion, namely the H(CH₃OH)₃⁺ cation, which has a similar *cba* band and has been characterized by X-ray crystallography.

The structure of the H(CH₃OH)₃⁺ cation in crystalline H(CH₃OH)₃⁺{Cl₁₁[−]} with O···O distances 2.446(2) and 2.491(2) Å is shown in Figure 14. The overall average O···O distance of 2.455 Å is close to the average of 2.481 Å in the nearly symmetrical H₇O₃⁺ cation in [H₇O₃⁺][H₉O₄⁺]⁺Br₂[−]·H₂O.⁵⁶ The spectra of the H(CH₃OH)₃⁺ cation in benzene solution and in the crystal phase as the {Cl₁₁[−]} salt are essentially the same, so the structure of the cation must be very similar in both phases.

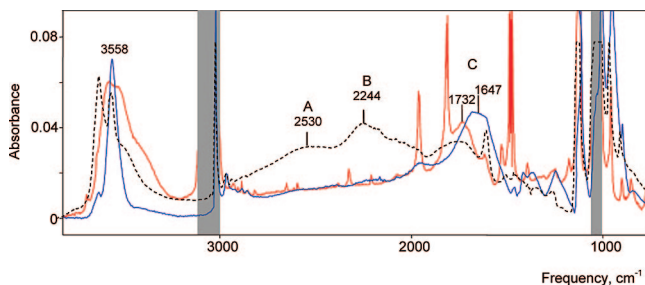


Figure 13. Comparison of the IR spectrum of α -H₇O₃⁺ cation in benzene solution (red) with those of solid H(CH₃OH)₃⁺{Cl₁₁[−]} (blue) and crystalline H₇O₃⁺{Cl₁₁[−]} (black dashed). The red and black spectra are normalized to unit absorption of the {Cl₁₁[−]} anion.

Since the O···O distances in the H(CH₃OH)₃⁺ cation are shorter than those in compounds containing isolated O–H···O groups (Table 2), the νOH frequency (*cba* center of gravity, $1920 \pm 40 \text{ cm}^{-1}$) is lower than, for example, that in phosphinic acid dimers ($2000\text{--}2070 \text{ cm}^{-1}$).⁴⁵ Comparing the spectrum of the H(CH₃OH)₃⁺ cation with that of the α -H₇O₃⁺ cation in benzene solution (Figure 13), close similarity can be seen.

The bands at ~ 1300 and 1732 cm^{-1} in the α -H₇O₃⁺ cation correspond to those at ~ 960 and $\sim 1655 \text{ cm}^{-1}$ in H(CH₃OH)₃⁺, and the center of gravity of the *cba* of α -H₇O₃⁺ practically coincides with that of H(CH₃OH)₃⁺, but for β -H₇O₃⁺ it is higher (Table 3). Therefore, the O···O distance of α -H₇O₃⁺ must be close to that of 2.455 Å in the H⁺(CH₃OH)₃ cation, while that in β -H₇O₃⁺ must be longer, approaching the value of 2.481 Å observed in the H₇O₃⁺ ion of [H₇O₃⁺][H₉O₄⁺]⁺Br₂[−]·H₂O. This demonstration of diminished H-bond strength in the (O···H–O–H···O)⁺ group of β -H₇O₃⁺ compared to that in H(CH₃OH)₃⁺ can be understood in terms of the weaker intrinsic basicity of water versus methanol. Nevertheless, the availability of five terminal OH groups in H₇O₃⁺ instead of two in H(CH₃OH)₃⁺ for H-bonding with the environment must also play an important role. The H₇O₃⁺ cation can more effectively transfer positive charge from the (O···H–O–H···O)⁺ group to the environment via a greater number of H-bonds.

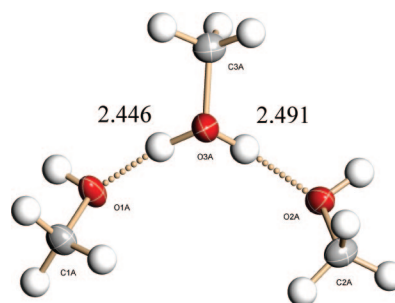


Figure 14. X-ray crystal structure of one cation of [H(MeOH)₃][CHB₁₁Cl₁₁] in the unit cell. Thermal ellipsoids are shown at the 50% probability level.

Table 3. νOH of H(H₂O)_{*n*}⁺ and H(CH₃OH)₃⁺ Cations Determined from the *cba* Center of Gravity

sample	solvent	νOH
α -H ₇ O ₃ ⁺ {Cl ₁₁ [−] }	benzene	1911 ± 40
α -H ₇ O ₃ ⁺ {H ₅ Br ₆ [−] }	DChE	2110 ± 40
β -H ₇ O ₃ ⁺ {H ₅ Br ₆ [−] }	DChE	2285 ± 40
H ₃ O ⁺ (H ₂ O) ₃ {Cl ₁₁ [−] }	crystal	2390 ± 40
H ₇ O ₃ ⁺ ·H ₂ O{Cl ₁₁ [−] }	benzene	2270 ± 40
H(CH ₃ OH) ₃ ⁺ {Cl ₁₁ [−] }	benzene	1920 ± 40

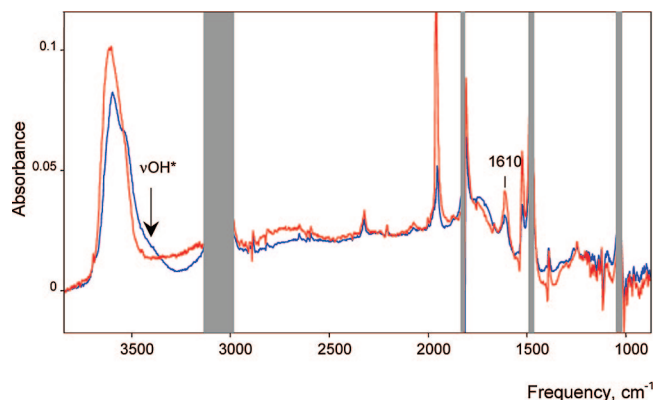
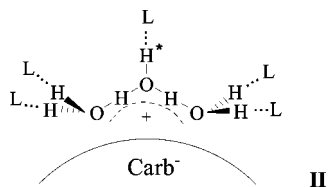
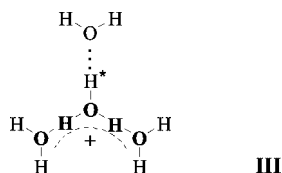


Figure 15. Spectrum of $H(H_2O)_4^+$ (red) compared to that of $\beta\text{-}H_7O_3^+$ (blue) after subtraction of solvent (benzene) and counterion $\{Cl_{11}^-\}$.

A weak blue shift of the *cba* center of gravity and the νOH frequencies of the terminal OH groups of the β isomer of $H_7O_3^+$ compared to those for the α isomer (Tables 1 and 3) indicate a slight weakening of both the internal $O\cdots H-O-H\cdots O$ core H-bonds and the external H-bonds with the environment in the β isomer. This may reflect different $H_7O_3^+$ /anion interactions. If aggregates of $\alpha\text{-}H_7O_3^+\{Cl_{11}^-\}$ ion pairs are associated with $H_5O_2^+\{Cl_{11}^-\}$ ion pairs, $\alpha\text{-}H_7O_3^+$ may experience a more spherically symmetric anion field than the unidirectional field of the simple ion-paired structure of $\beta\text{-}H_7O_3^+\{Cl_{11}^-\}$. As shown schematically by **II**, the polarization of the β cation by the anion weakens its interaction with the environment.

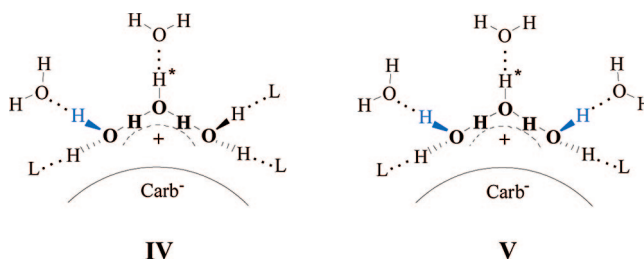


$H(H_2O)_n^+$ Cations with $n \geq 4$. The formation of the $H(H_2O)_4^+$ cation as an individual entity is detected with higher certainty in the lower permittivity solvent, benzene, rather than DCE. As shown in Figure 15, its IR spectrum is very similar to that of $\beta\text{-}H_7O_3^+$. The two differences are that (a) the νOH^* band of the “free” OH^* group at 3458 cm^{-1} is red-shifted to the region of $\sim 3200\text{ cm}^{-1}$, and (b) there is an increase in the intensity of the $\nu_{\text{as}}\text{H}_2\text{O}$, $\nu_{\text{s}}\text{H}_2\text{O}$, and $\delta\text{H}_2\text{O}$ (1610 cm^{-1}) bands from an added peripheral H_2O molecule. These changes are readily understood in terms of structure **III**. Compared to $H_7O_3^+$, the OH^* group



is now H-bonded to H_2O rather than solvent, so the νOH^* frequency is decreased. The fourth water molecule is not equivalent to the other two peripheral H_2O groups, and $\nu_{\text{as}}\text{H}_2\text{O}$ and $\nu_{\text{s}}\text{H}_2\text{O}$ develop as one broad, asymmetric band. The absorptions from the core $(O\cdots H-O-H\cdots O)^+$ group are nearly unchanged, indicating that the $H_7O_3^+$ ion remains the fundamental building block. The $H_7O_3^+-\text{H}_2\text{O}$ interaction is relatively weak, so the $H(H_2O)_4^+$ cation is more correctly represented as the monohydrated $H_7O_3^+$ cation, i.e., $H_7O_3^+\cdot\text{H}_2\text{O}$.

As noted earlier, the close similarity of the spectroscopic properties of $H(H_2O)_n^+$ cations with $n \geq 4$ means that these cations all belong to one family of compounds. Their spectra show isobestic points, and the only significant differences arise from absorptions from the increasing number of peripheral water molecules (Figure 16). All the data can be rationalized by the sequential attachment of three water molecules to the $H_7O_3^+$ cation in structures **III**, **IV**, and **V** for $n = 4, 5$, and 6 , respectively ($L = \text{solvent}$). In each cation, the $(O\cdots H-O-H\cdots O)^+$ structural unit of the $H_7O_3^+$ ion is retained as the basic building block.



Consistent with these structures, only the spectra for $N = 5$ and 6 show an increase in intensity of the broad band νOH at 3327 cm^{-1} (Figure 16) arising from the H-bonded OH groups of semihydrated water molecules (designated earlier as type (ii) and indicated in blue in **IV** and **V**). This is accompanied by a Fermi resonance band at 3180 cm^{-1} from the overtone of $2\delta\text{H}_2\text{O}$. Finally, the constancy of the $\delta\text{H}_2\text{O}$ frequency at $1608\text{--}1610\text{ cm}^{-1}$ for all cations with $n = 3\text{--}6$ is in agreement with structures **IV** and **V**, since they contain closely related peripheral water molecules only of types (i) and (ii).

The $H(H_2O)_6^+$ cation with $\{H_5Br_6^-\}$ counterion is formed in DCE solution under conditions of water saturation. However, by using alternative carborane acids and extracting them from aqueous solution at varying temperatures, $H(H_2O)_n^+$ cations with $n > 6$ may be obtained. Figure 17 presents the spectra of cations from aqueous $H\{\text{CCD}\}$ extracts with N varying from $5.5\text{--}6.5$, as well as the spectrum of an $H\{I_{11}\}$ extract in which N reaches 8.2 . In all spectra, the absorptions from the core $(O\cdots H-O-H\cdots O)^+$ group remain unchanged, as indicated by the constancy of the *cba* from 3000 to 1500 cm^{-1} .

Let us now consider the interaction between the terminal water molecules and $H_7O_3^+$ group in more detail. Figure 18 shows the difference spectrum of cations with $n = 4$ and 4.74 in order to reveal the bands associated with the fifth added water molecule. The $\nu_{\text{as}}\text{H}_2\text{O}$ band appears at 3650 cm^{-1} , the lower frequency $\nu_{\text{s}}\text{H}_2\text{O}$ band is masked by other νOH vibrations, and the νOH band from the OH group of the $H_7O_3^+$ cation to which the fifth H_2O molecule is H-bonded (type (ii), marked blue in **IV**) appears at 3350 cm^{-1} . A small shift in the *cba* to higher frequency (in the range of the A band) results in a broad band at 2980 cm^{-1} . With the exception of a weak $\delta\text{H}_2\text{O}$ band from the fifth H_2O molecule, there are no changes below 2500 cm^{-1} . Similar difference spectra of cations are obtained with $n = 6$ (counterion $\{\text{CCD}^-\}$, DCE) and $n = 5.2$ (counterion $\{H_5Br_6^-\}$, DCE), except that the relative intensity of the band at 2980 cm^{-1} is weaker. So all changes in the spectra are in accordance with structures **III**, **IV**, and **V**. In the difference spectra of cations with $n = 6.5$ and 5.5 (DCE, CCD^- as counterion), the intensities of the bands at 3655 , 3400 , and 1608 cm^{-1} increase in accordance with additional water molecules of type (i) or (ii). The *cba* is not changed. However, for the first time, a $\delta\text{H}_2\text{O}$ band appears at $\sim 1630\text{ cm}^{-1}$ (Figure 17 inset). This is assigned

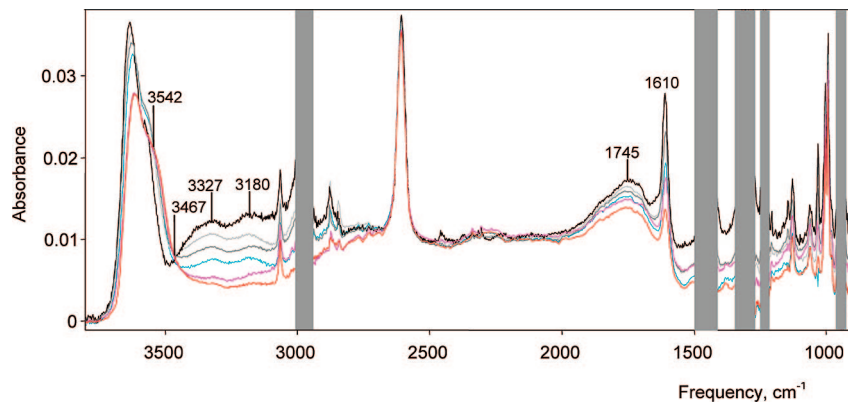
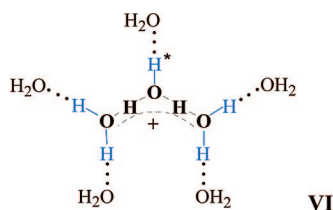
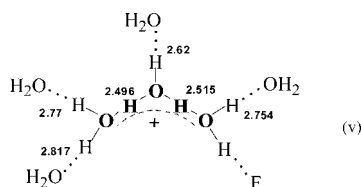


Figure 16. IR spectra (red through black) of DCE solutions of $\text{H}(\text{H}_2\text{O})_n^+ \{\text{H}_5\text{Br}_6^-\}$ with $n = 3.02, 3.1, 3.4, 3.7, 4.2,$ and 5.2 .

to water molecules of type (iii) having both OH groups H-bonded to solvating H_2O molecules. A similar band with higher intensity appears in the difference spectrum of cations with $n = 8-9$ and $n = 5.5$. Thus, attachment of the seventh and eighth water molecules to the $\text{H}(\text{H}_2\text{O})_6^+$ cation leads to cation **VI**.



The structure of the $\text{H}(\text{H}_2\text{O})_7^+$ cation has been determined by X-ray in the crystalline hydrate $\text{H}_2\text{SiF}_6 \cdot 9.5\text{H}_2\text{O}$.⁵⁷ It comprises the H_7O_3^+ building block surrounded with five H_2O molecules and one F atom from a SiF_6^{2-} anion as shown in (v).



This is very similar to structure **VI** proposed for $\text{H}(\text{H}_2\text{O})_8^+$ in solution. The $\text{O}\cdots\text{O}$ distances in the $\text{O}\cdots\text{H}-\text{O}-\text{H}\cdots\text{O}$ group of (v) are lengthened to $2.505(2)$ Å, compared with the average of 2.481 Å in $[\text{H}_7\text{O}_3^+][\text{H}_9\text{O}_4^+]\text{Br}^-_2 \cdot \text{H}_2\text{O}$ (iv), where the H_7O_3^+ ion is bonded with only two water molecules. It is evident that increasing the number of H-bonded water molecules solvating the H_7O_3^+ cation delocalizes the positive charge and weakens H-bonding in the core $\text{O}\cdots\text{H}-\text{O}-\text{H}\cdots\text{O}$ unit. The 2.505 Å $\text{O}\cdots\text{O}$ distance is close to that in dimers of dialkylphosphinic acids ($2.51-2.52$ Å), which is why their *cba*'s are quite similar. Structure v reflects the weak H-bonding between the H_7O_3^+ cation and three solvating water molecules ($R_{\text{O}\cdots\text{O}} = 2.77-2.81$ Å). They are comparable to those in neutral liquid water ($R_{\text{O}\cdots\text{O}} = 2.78$ Å).⁵⁸ The OH^* group forms a somewhat stronger H-bond, with $R_{\text{O}\cdots\text{O}} = 2.62$ Å, which nevertheless is insufficient to contribute to the *cba* below 2600 cm^{-1} .

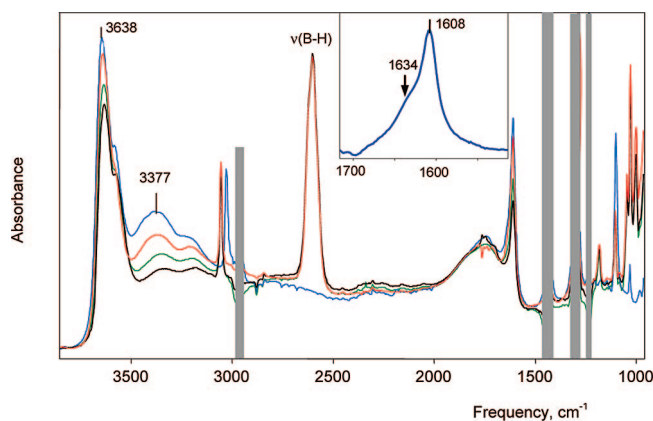


Figure 17. IR spectra of $\text{H}(\text{H}_2\text{O})_n^+$ cations in water-saturated DCE: black, $N = 5.5$; green, $N = 6.0$; red, $N = 6.5$; blue, $N = 8.2$. The anion is $\{\text{CCD}\}^-$ in the black, green, and red spectra and $\{\text{I}_{11}\}^-$ in the blue. In the inset, the difference of the spectra with $N = 8.2$ and 5.5 is given to show, with higher certainty, the appearance of the $\delta\text{H}_2\text{O}$ band at 1634 cm^{-1} of the water molecules of type (iii) in cation **VI**.

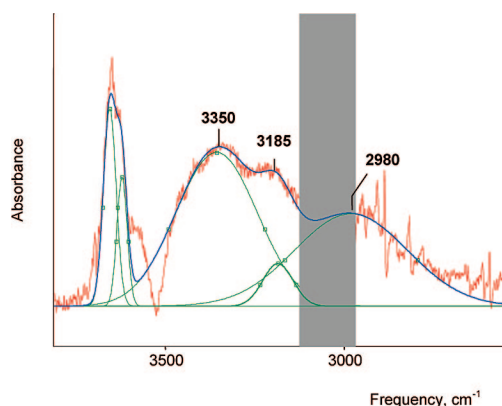


Figure 18. Deconvolution of the difference spectrum between cations with $N = 4.52$ and $N = 4$ for benzene solution (counterion $\{\text{Cl}_{11}\}^-$).

Comparison with Gas and Solid Phases. The structures of $\text{H}(\text{H}_2\text{O})_n^+$ cations in acidified organic solutions are similar to those in the gas phase only when $n = 1, 2, 7, 9$ and 3 . For $n \geq 4$, they can be quite different. In the gas phase, the Gibbs energy dependence of the addition of the n th molecule of H_2O to the $\text{H}(\text{H}_2\text{O})_{n-1}^+$ hydrate indicates extra stability of the $\text{H}(\text{H}_2\text{O})_4^+$ and $\text{H}(\text{H}_2\text{O})_6^+$ cations.¹³ Indeed, the stability of $\text{H}(\text{H}_2\text{O})_4^+$ is higher than that of H_7O_3^+ . In organic solvents, the situation is different. The stability of H_3O^+ , H_5O_2^+ , and H_7O_3^+ is high, but starting with the $\text{H}(\text{H}_2\text{O})_4^+$ cation, stability

(56) Lundgren, J.-O.; Olovsson, I. *J. Chem. Phys.* **1968**, *49*, 1068–1074.
 (57) Mootz, D.; Oellers, E.-J. *Z. Anorg. Allg. Chem.* **1988**, *559*, 27–39.
 (58) Head-Gordon, T.; Hura, G. *Chem. Rev.* **2002**, *102*, 2651–2670.

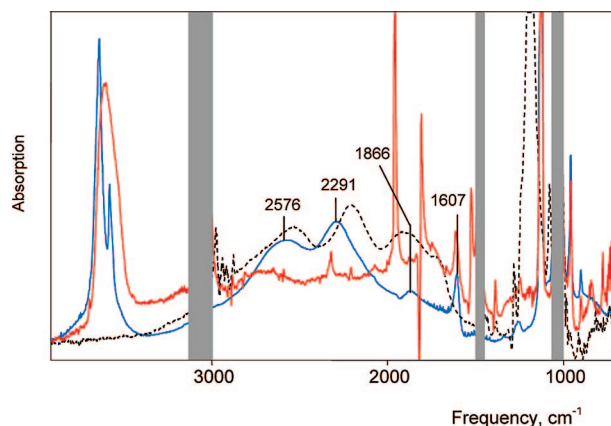
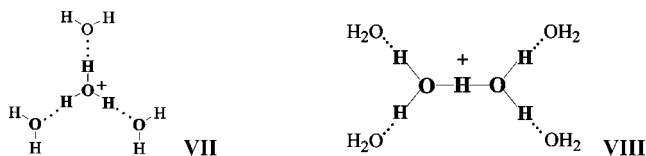


Figure 19. IR spectra of $H(H_2O)_4^+\{Cl_{11}\}^-$ ($N = 3.91$) in benzene (red), crystalline $[H_3O^+\cdot 3H_2O]\{Cl_{11}\}^-$ (blue), and $[H_3O^+\cdot 3TBP]FeCl_4^-$ in CCl_4 (black dashed). Red and blue are normalized to unit intensity of anion.

sharply decreases without any particular stability of cations with further increasing n .

In accordance with quantum mechanical calculations^{10,19,59} and confirmed by IR spectroscopy,^{10,19} the most stable structures for the $H(H_2O)_4^+$ and $H(H_2O)_6^+$ cations *in vacuo* are symmetrical structures **VII** and **VIII**, respectively. However, some calculations (G3B3 and CBS-QB3²² or DFT²¹) predict a slightly higher stability for structure **V** compared to **VIII** for $H(H_2O)_6^+$ cation. Their energy difference is so small that both **V** and **VIII** may coexist. In any case, cations $H_3O^+\cdot 3H_2O$ (**VII**) and $H_5O_2^+\cdot 4H_2O$ (**VIII**) have also been characterized in the solid phase by X-ray diffraction.^{60,61}



The gas-phase spectrum of **VII** develops two bands, $\nu_s H_2O = 3644$ and $\nu_{as} H_2O = 3730$ cm^{-1} , from the three equivalent H_2O molecules surrounding the H_3O^+ ion and a broad band of ν_{as} and ν_s at 2665 cm^{-1} for the central H_3O^+ .¹⁰ In the crystalline state of $[H_3O^+\cdot 3H_2O]\{Cl_{11}\}^-$, the OH stretch frequencies from H_3O^+ occur as a coalesced broad band at lower frequency, 2576 cm^{-1} (Figure 19), because the three H-bonded water molecules are made more basic by the anion environment. A combination band appears at 2291 cm^{-1} . The frequencies of the three terminal water molecules of $H_3O^+\cdot 3H_2O$ appear at ν_{as} 3637 , ν_s 3578 , and δH_2O 1605 cm^{-1} bands. In the low-frequency region, a weak band appears ~ 1200 cm^{-1} , possibly $\nu_2 H_3O$, overlapped with strong bands from counterion. The spectrum is also very similar to that of the C_{3v} -symmetric $H_3O^+\cdot 3TBP$ cation, an analogue of **VII**.²⁷ The slightly higher basicity of TBP compared to H_2O results in a small red-shift of νOH to 2530 cm^{-1} and the combination band to 2206 cm^{-1} .

Comparing the spectrum of the symmetrical $H(H_2O)_4^+$ cation in $[H_3O^+\cdot 3H_2O]\{Cl_{11}\}^-$ with that in solution reveals differences ascribable to different structures: the symmetrical Eigen-type $H_3O^+\cdot 3H_2O$ cation in the crystal and the less symmetrical

$H_7O_3^+\cdot H_2O$ cation in benzene or DCE solution (Figure 19). They show some similarities in the *cba* region, originating from conjugated $O-H\cdots O$ group vibrations, but nevertheless there are important distinctions in the distribution of the *cba* intensity that defines the νOH frequencies. For the $H_7O_3^+\cdot H_2O$ cation in benzene solution, νOH is about 120 cm^{-1} lower than in the $H_3O^+\cdot 3H_2O$ cation (Table 3). This reflects shorter $O\cdots O$ distances in the $O\cdots H-O-H\cdots O$ core of the $H_7O_3^+\cdot H_2O$ cation compared to $O-H\cdots O$ in $H_3O^+\cdot 3H_2O$. In the X-ray structure of $[H_7O_3^+][H_9O_4^+]Br_2\cdot H_2O$,⁵⁶ where both cations appear in the same crystal, this difference is $2.48(1)$ versus $2.56(1)$ Å (averaged over equivalent bonds). The average $O\cdots O$ distance in the $H_3O^+\cdot 3H_2O$ cation is $2.51(2)$ Å⁶⁰ with $\{H_3Br_6\}^-$ as counterion and $2.530(2)$ Å with $\{Cl_{11}\}^-$.

Similarly, a comparison of the $H(H_2O)_6^+$ cation in solution versus the gas phase or a symmetrical crystal environment reveals considerable structural differences. For the gas phase, the measured and calculated IR spectra provide evidence that the $H(H_2O)_6^+$ cation has a $H_5O_2^+$ core.^{10,19} However, other calculations based on different levels of theory predict that the lowest energy state *in vacuo* of the tetrahydrated $H_5O_2^+$ ion, namely $H_5O_2^+\cdot 4H_2O$ cation **VIII**, is insignificantly lower (or even higher) than that for the $H_7O_3^+\cdot 3H_2O$ ion (**V**).^{21,22} For the crystal state, only one example of a type **VIII** cation is known. It is found in the strictly symmetric Cl^- anion environment of a cage compound, $[(C_9H_{18})_3(NH_2)_2Cl]Cl^-$, crystallized from HCl solution.⁶¹ In the solutions of the present study, the IR data on $H(H_2O)_6^+$ retain the characteristics of the $H_7O_3^+$ core, indicating formulation as the $H_7O_3^+\cdot 3H_2O$ ion, structure **V**. Since the vibrations of the $O\cdots H-O-H\cdots O$ core of $H_7O_3^+\cdot nH_2O$ cations in solution with $n \geq 6$ are very similar to those from the $O-H\cdots O$ group of phosphinic acid dimers, the $O\cdots O$ distances should be similar. They are ~ 2.49 – 2.53 Å for phosphinic acid dimers.^{46,47,62} The average $O\cdots O$ distance in the core of the $H_7O_3^+\cdot 4H_2O$ cation in the SiF_6^{2-} salt is 2.505 Å.⁵⁷ Therefore, in $H(H_2O)_n^+$ cations with $n \geq 6$ in solution, the $O\cdots O$ distances should be ca. 2.51 Å. By comparison, the central $O\cdots O$ distance in $H_5O_2^+\cdot 4H_2O$ should be ca. $2.39(2)$ Å, as in crystal state.⁶¹ This distance is typical for $L-H^+-L$ proton disolvates with strong L bases, such as diethyl ether.^{54,63} These cations, including $H_5O_2^+$, develop intense bands in the 800 – 1000 cm^{-1} region from $O-H^+-O$ group vibrations.^{7,54,63} In accordance with DFT/B3LYP and MP2 calculations,⁶⁴ complexation of the $H_5O_2^+$ cation with four H_2O molecules only marginally influences the frequency and strong intensity of these bands. However, they are absent in the spectra of $H_7O_3^+\cdot 3H_2O$ in solution.

Thus, the Eigen- and Zundel-type symmetrical cations $H_3O^+\cdot 3H_2O$ (**VII**) and $H_5O_2^+\cdot 4H_2O$ (**VIII**) exist in the gas phase where counterions are absent. Rare cases also exist in the solid phase where the cation happens to be nearly symmetrically surrounded by anions or other ligands. In solutions with aprotic solvents such as benzene and chlorinated hydrocarbons, the one-dimensional electrostatic influence of the anion in solvent-separated ion pairs results in higher stability of the $H_7O_3^+\cdot H_2O$ cation with structure **III** and $H_7O_3^+\cdot 3H_2O$ with structure **V**.

(59) Christie, R. A.; Jordan, K. D. *J. Phys. Chem. B* **2002**, *106*, 8376–8381.

(60) Xie, Z.; Bau, R.; Reed, C. A. *Inorg. Chem.* **1995**, *34*, 5403–5404.

(61) Bell, R. A.; Christoph, G. G.; Fronczek, F. R.; Marsh, R. E. *Science* **1975**, *190*, 151–152.

(62) Reis, A. H.; Peterson, S. W.; Druyan, M. E.; Gebert, E.; Mason, G. W.; Peppard, D. F. *Inorg. Chem.* **1976**, *15*, 2748–2752.

(63) Stoyanov, E. S. *Phys. Chem. Chem. Phys.* **2000**, *2*, 1137–1145.

(64) Sobolewski, A. L.; Domcke, W. *J. Phys. Chem. A* **2002**, *106*, 4158–4167.

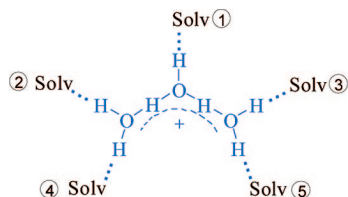
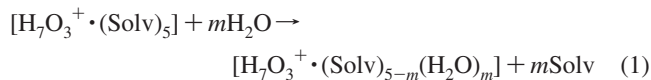


Figure 20. $\text{H}_7\text{O}_3^+(\text{Solv})_5$ cation, showing the structurally distinct sites of the first solvation shell. Site 1 is hydrated first, and then sites 2 and 3, and finally sites 4 and 5.

The present results better allow us to appreciate the similarities and differences of the excess proton in water versus methanol.³³ In benzene solution with carborane counterions, the $\text{H}(\text{H}_2\text{O})_n^+$ and $\text{H}(\text{CH}_3\text{OH})_n^+$ cations have similar spectra and structures for $n = 2$ and 3. At $n = 4$, however, different core structures become the building blocks for higher solvation. This occurs because the $\text{O}-\text{H}^*$ group in H_7O_3^+ is replaced by an $\text{O}-\text{CH}_3$ group in $\text{H}(\text{CH}_3\text{OH})_3^+$ and is therefore unavailable for H-bonding. Water clusters can grow in dendritic fashion, whereas methanol clusters are forced to grow as linear chains. As a result, methanol clusters grow linearly as unique cations up to $n = 4$, each with individual spectral properties. Solvation continues up to $n = 8$ chains, retaining the properties of the $\text{H}(\text{CH}_3\text{OH})_4^+$ core.³³ On the other hand, water clusters cease to develop unique cations after $n = 3$, retaining the H_7O_3^+ core.

Conclusions

Study of the stepwise bonding of water molecules to H^+ in weakly basic solvents with weakly basic anions shows that the first three hydrates, namely H_3O^+ , H_5O_2^+ , and H_7O_3^+ , behave as individual ions with unique and distinctive structures and IR spectra. Additional water molecules are H-bonded to the H_7O_3^+ cation via stepwise replacement of organic solvent molecules from its first coordination sphere via eq 1 and Figure 20.



Hydration of the $\text{H}_7\text{O}_3^+(\text{Solv})_5$ ion occurs first at the strongest coordination position, site 1. The second and third H_2O molecules replace solvent molecules at positions 2 and 3, forming the $\text{H}^+(\text{H}_2\text{O})_6$ cation, which is stable with all studied counterions in both benzene and DCE. Finally, with some of the studied counterions in DCE solvent, two further H_2O molecules can be introduced in positions 4 and 5, to form the less stable $\text{H}^+(\text{H}_2\text{O})_8$ cluster, completing the first coordination sphere of H_7O_3^+ cation. There are detectable changes in the

spectrum of the H_7O_3^+ ion as it is solvated by 1–3 water molecules, but the core structure is retained for all m . Comparisons of IR data and X-ray data lead to the conclusion that, in $\text{H}(\text{H}_2\text{O})_n^+$ cations with $n > 4$, the two $\text{O}\cdots\text{O}$ distances in the conjugated $\text{O}\cdots\text{H}-\text{O}-\text{H}\cdots\text{O}$ group, where the excess proton resides, are ca. 2.51 Å.

Notably, neither Eigen-type structures with the H_3O^+ core nor Zundel-type structures with the H_5O_2^+ core are present. This finding is contrary to popular expectation and contrary to calculation and experiment in the gas phase. It reflects the unfortunate fact that perceptions regarding the nature of the aquated proton in solution have become too biased by calculations and experiments in the gas phase, where counterions are absent. The present work suggests that the obligatory presence of a counterion in solution, no matter how weakly coordinating, exerts an anisotropic electrostatic influence on $\text{H}(\text{H}_2\text{O})_n^+$ cations that has been largely ignored. The presence of the conjugate base of the acidic $\text{H}(\text{H}_2\text{O})_n^+$ cations is the principal reason that different structures exist in the condensed phase *vis à vis* the gas phase. The question about where the positive charge is localized has been typically been phrased in terms of Eigen and/or Zundel type ions, i.e., on one water molecule or shared between two. For the presently studied $\text{H}(\text{H}_2\text{O})_n^+$ clusters, the excess proton is localized between *three* oxygen atoms, and the positive charge influences up to six water molecules. Additional water molecules above $n = 6$ are essentially indistinguishable from bulk water.

The next challenge will be to determine experimentally the nature of $\text{H}(\text{H}_2\text{O})_n^+$ in liquid water. Most theory focuses on Eigen versus Zundel ions,^{11,12} or a continuum of structures in between,⁶⁵ although one study favors H_7O_3^+ as the major ion present.⁶⁶ The present work provides an excellent experimental fingerprint for this ion.

Acknowledgment. We thank Drs. Kee-Chan Kim for experimental assistance and the National Science Foundation (CHE-039878) and the National Institutes of Health (GM 23851) for support.

Supporting Information Available: Additional characterization and crystallographic data (PDF, CIF). This material is available free of charge via the Internet at <http://pubs.acs.org>.

JA803535S

(65) Bush, V.; Dubrovsky, A.; Mohamed, F.; Parrinello, M.; Sadlej, J.; Hammerich, A. D.; Devlin, J. P. *J. Phys. Chem. A* **2008**, *112*, 2144–2161.

(66) Heuft, J. M.; Meijer, E. J. *Phys. Chem. Chem. Phys.* **2006**, *8*, 3116–3123.